Available online at www.sciencedirect.com
ScienceDirect
Journal of Hazardous Materials 154 (2008) 595–601
Journal of Hazardous Materials
www.elsevier.com/locate/jhazmat

Adsorption of organic pollutants from coking and papermaking wastewaters by bottom ash

Wei-ling Sun *, Yan-zhi Qu, Qing Yu, Jin-ren Ni

Department of Environmental Engineering, Peking University, The Key Laboratory of Water and Sediment Sciences, Ministry of Education, Beijing 100871, China

Received 26 July 2007; received in revised form 18 October 2007; accepted 18 October 2007
Available online 24 October 2007

Abstract

Bottom ash, a power plant waste, was used to remove the organic pollutants in coking wastewater and papermaking wastewater. Particular attention was paid on the effect of bottom ash particle size and dosage on the removal of chemical oxygen demand (COD). UV–vis spectra, fluorescence excitation-emission matrix (FEEM) spectra, Fourier transform infrared (FTIR) spectra, and scanning electron microscopic (SEM) photographs were investigated to characterize the wastewaters and bottom ash. The results show that the COD removal efficiencies increase with decreasing particle sizes of bottom ash, and the COD removal efficiency for coking wastewater is much higher than that for papermaking wastewater due to its high percentage of particle organic carbon (POC). Different trends of COD removal efficiency with bottom ash dosage are also observed for coking and papermaking wastewaters because of their various POC concentrations. Significant variations are observed in the FEEM spectra of wastewaters after treatment by bottom ash. New excitation-emission peaks are found in FEEM spectra, and the fluorescence intensities of the peaks decrease. A new transmittance band in the region of 1400–1420 cm^{-1} is observed in FTIR spectra of bottom ash after adsorption. The SEM photographs reveal that the surface of bottom ash particles varies evidently after adsorption.

Keywords: Adsorption; Bottom ash; Coking wastewater; Papermaking wastewater; Organic pollutants

1. Introduction

The treatment of coking wastewater and papermaking wastewater poses considerable problems in the wastewater treatment industry. It is difficult to remove the complex inorganic and organic contaminants because most of these compounds are refractory, highly concentrated, toxic, mutative and carcinogenic and may produce long-term environmental and ecological impacts [1]. Furthermore, conventional biological and chemical processes are insufficient in removing these contaminants [2], and more efforts on advanced processes for coking and papermaking wastewaters treatment are still necessary to reduce the discharge of contaminants and their adverse effect on environment. Adsorption technique is being widely used for wastewater treatment due to its versatile and efficient ability to separate a wide range of chemical compounds, and easily operational procedures [3].

Bottom ash, a kind of waste material generated from thermal coal-fired power plants, is generally used in road bases and building materials. In some areas, proper disposal of bottom ash has been a cause of worry to the local governments due to its excessive amount [4]. Recently, there is growing interest in bottom ash utilization, particularly in the waste management, where bottom ash is often used as a sorbent for various pollutants especially in water [3–14]. It has been found that bottom ash has good efficacy to remove dyes from aqueous solution, such as Quinoline Yellow [3], Brilliant Blue FCF [4], malachite green [5], Amaranth [6], Acid Orange 7 [7], Tartrazine [8], indigo carmine [9], erythrosine [10], Vertigo Blue 49 and Orange DNA 13 [11], Methyl Orange [12], Methyl Violet [13], and Metanil Yellow [14]. However, most of these previous researches are limited in the synthetic wastewaters. Few studies were conducted using bottom ash for removal of organic pollutants in practical wastewaters.

To develop a more suitable, efficient, cheap and easily accessible type of adsorbent, an attempt was made in this research to use bottom ash for removal of organic pollutants in coking wastewater and papermaking wastewater. Particular attention

* Corresponding author. Tel.: +86 10 62767014; fax: +86 10 62767014.
E-mail address: sunweiling@iee.pku.edu.cn (W.-l. Sun).

0304-3894/$ – see front matter © 2007 Elsevier B.V. All rights reserved.
doi:10.1016/j.jhazmat.2007.10.063

Table 1
Water quality of coking and papermaking wastewaters

Wastewater	pH	COD (mg/L)	TOC[a] (mg/L)	NH_3-N[b] (mg/L)	TN[c] (mg/L)	TP[d] (mg/L)	Color (°)
Coking	8.75	112.0	38.62	4.53	22.80	0.95	125
Papermaking	8.73	67.2	15.47	0.60	2.06	0.62	ND[e]

[a] TOC: total organic carbon.
[b] NH_3-N: ammonium nitrogen.
[c] TN: total nitrogen.
[d] TP: total phosphorus.
[e] ND: undetected.

was paid on the effect of bottom ash particle size and dosage on the removal of chemical oxygen demand (COD). Characterizations of wastewater and bottom ash were made by UV–vis spectra and fluorescence excitation–emission matrix (FEEM) spectra, and Fourier transform infrared (FTIR) spectra and scanning electron microscopic (SEM) photographs, respectively.

2. Materials and methods

2.1. Raw wastewater

The coking wastewater used in the experiments was collected from the effluent of a coke plant in Shanxi province with the treatment processes of anaerobic–aerobic biological treatment and zero-valent iron treatment. The papermaking wastewater was sampled from the outlet of the papermaking wastewater treatment plant of the Gold East Paper Co., Ltd., located in Zhenjiang city, Jiangsu province. The papermaking wastewater was subjected to primary clarifier, activated sludge process, and final clarifier in the wastewater treatment plant. Table 1 shows the special chemical parameters of the wastewater samples used in the experiments.

2.2. Bottom ash preparation

Bottom ash was obtained from thermal power station (TPS) of Gold East Paper Co., Ltd. The coal used by TPS of Gold East Paper Co., Ltd. was obtained from Shanxi province, and the sulfur and ash contents of the coal are less than 1% and 15%, respectively. The samples were ground and screened to give different particle sizes such as 2.0–6.0 mm, 1.0–2.0 mm, 0.45–1.0 mm, 0.2–0.45 mm, 0.074–0.2 mm, and <0.074 mm. The chemical composition, surface area, and mineral components of bottom ash were analyzed using X-ray fluorescence spectrometer (ARL ADVANT'XP, Thermo Electron, USA), surface area analyzer (ST-03, Beijing Analytical Instruments Company, China), and X-ray diffractophotometer (D/max-RA, Rigaku, Japan), respectively. The results are shown in Table 2.

2.3. Influence of particle size and dosage

To examine the effect of particle size, 5 g of bottom ash with a specific particle size was added into a 100 mL triangular flask, and 50 mL wastewater was added. To investigate the influence of bottom ash dosage, different quantities of bottom ash were added into a 100 mL triangular flask, and 50 mL wastewater was poured.

All the experiments were carried out in a water-bath shaker for 3 h at 25 ± 1 °C. Preliminary experiments showed that the adsorption equilibrium is reached in 3 h. After equilibrium, the water samples were centrifugated at 5000 rpm for 15 min, and then the supernate was analyzed further.

All the experiments were performed in duplicate, and the mean value of the parallel samples was calculated.

2.4. Analytical method

COD of wastewater samples was measured by the potassium dichromate oxidation method (Hach Heating System, Hach Corporation, USA). The Color of wastewaters was determined using dilution method. TOC of wastewater samples was analyzed by Muti TOC/TN 3000 Analyzer (Analytic Jena, Germany), and dissolved organic carbon (DOC) was determined after filtration through a 0.45 μm pore size filter membrane. Particle organic carbon (POC) was calculated by the difference between TOC and DOC.

The UV–vis absorption spectra of wastewaters were measured from 200 nm to 800 nm using an UV-visible spectrophotometer (SPECORD 200, Analytik Jena, Germany) in a 1 cm quartz cell.

The FEEM spectra of the wastewater samples were recorded with F-4500 fluorometer (HITACHI, Japan). A 450-W Xenon lamp was used as the excitation source. FEEM were collected every 5 nm over an excitation (Ex) range of 200–500 nm, with an emission (Em) range of 250–600 nm by 5 nm. The spectra were obtained by subtracting Milli-Q water blank spectra, recorded under the same conditions, to eliminate water Raman scatter peaks.

Table 2
Characteristics of bottom ash

Chemical composition (wt.%)	Value	Mineral components (wt.%)	Value
SiO_2	51.87	Quartz	66
Al_2O_3	26.83	Mullite	10
Fe_2O_3	8.75	Potash feldspar	9
CaO	4.98	Plagioclase	4
K_2O	1.45	Calcite	2
TiO_2	1.54	Lime	2
MgO	0.41	Graphite	5
Others	4.17		
Surface area (m^2/g)	1.25		

The infrared spectra of bottom ash samples were recorded using a VECTOR22 FTIR spectrometer (Bruker, Germany) scanning over the frequency ranged from 4000 to 400 cm^{-1} at a resolution of 1 cm^{-1}. For the SEM analysis, Field-emission Scanning Electron Microscope (XL30SFEG, FEI, Netherlands) was employed.

3. Results and discussion

3.1. Effect of particle size

3.1.1. COD removal

In general, the COD removal efficiencies are found to increase with decreasing particle sizes of the bottom ash (Fig. 1) for coking wastewater and papermaking wastewater. This is consistent with the results observed by Gupta et al. [5], Gupta [7], and Mittal et al. [8,9,12–14]. The COD removal efficiency increases from 20.0% to 35.0% for coking wastewater, and from 5.3% to 11.1% for papermaking wastewater with the decrease of particle sizes from 2–6 mm to 0.074–0.2 mm. The COD removal efficiencies by <0.074 mm of bottom ash are 45.0% and 40.6%, respectively, for coking wastewater and papermaking wastewater. Moreover, the COD removal efficiencies for coking wastewater are much higher than those for papermaking wastewater. This may result from the various compositions of organic matters in coking wastewater and papermaking wastewater.

To investigate the composition of organic components in coking wastewater and papermaking wastewater, the 0.45 μm membrane was used to determine the concentrations of POC and DOC in wastewaters [15]. As shown in Fig. 2, the POC and DOC concentrations are 6.56 mg/L and 32.06 mg/L for coking wastewater, and 0.36 mg/L and 15.11 mg/L for papermaking wastewater. The percentage of POC in TOC is 17.0% for coking wastewater, and only 2.3% for papermaking wastewater. The POC is more easily removed than DOC by bottom ash. Therefore, the COD removal efficiency for coking wastewater is much higher than that for papermaking wastewater due to its high percentage of POC.

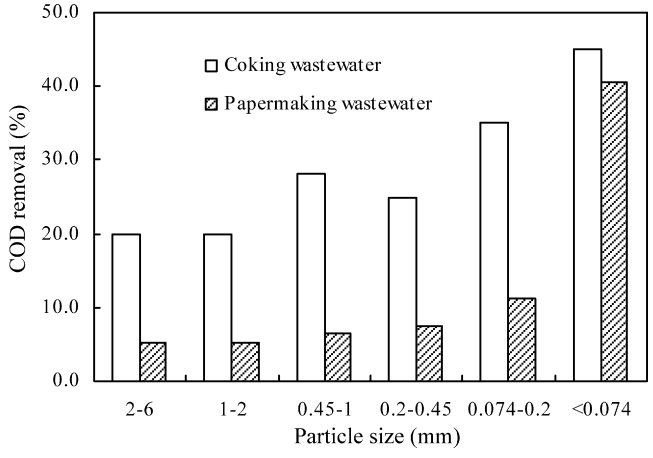

Fig. 1. COD removal efficiency for different particle sizes of bottom ash at 25 °C. Adsorbent dosage = 10 g/100 mL, pH = 8.75 (coking wastewater) and 8.73 (papermaking wastewater).

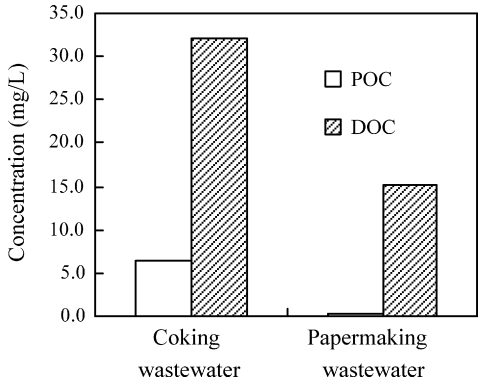

Fig. 2. POC and DOC distribution in coking and papermaking wastewaters.

3.1.2. Color and OM_{275} removal

Fig. 3 presents the UV–vis absorption spectra of coking wastewater and papermaking wastewater. An absorption band is observed in the UV region of 275 nm for the papermaking wastewater, while a weak absorption peak at 430 nm is found for the coking wastewater. The absorption in the UV region of 275 nm represents the abundance of aromatic rings in organic matter structure [16]. Absorbing light in the visible region (400–800 nm) means the compound looks colored. Fig. 3 reveals that there are aromatic chemicals in papermaking wastewater, and the color of the coking wastewater is visible. As illustrated in Table 1, the color of the coking wastewater is 125° (dilution factor).

The organic matters, absorbing UV-light at 275 nm, in papermaking wastewater is defined as OM_{275} here, and the removal efficiencies of color and OM_{275} were further analyzed for coking wastewater and papermaking wastewater respectively.

For coking wastewater (Fig. 4(a)), the color removal efficiency increases with decreasing particle sizes of bottom ash, and varies from 4.0% to 76.0% with particle sizes ranging from 2–6 mm to <0.074 mm. Furthermore, the removal efficiency of color is higher than that of COD for bottom ash with smaller particle sizes, and it is contrary for bottom ash with larger particle sizes. This implies greater effect of particle size on color removal than COD removal for coking wastewater.

For papermaking wastewater, the removal efficiency of OM_{275} increases slowly with the decrease of particle sizes

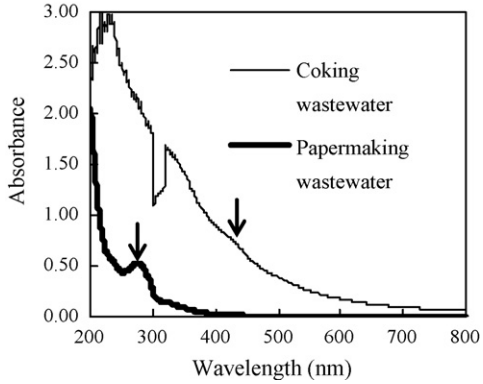

Fig. 3. UV–vis spectra of coking and papermaking wastewaters.

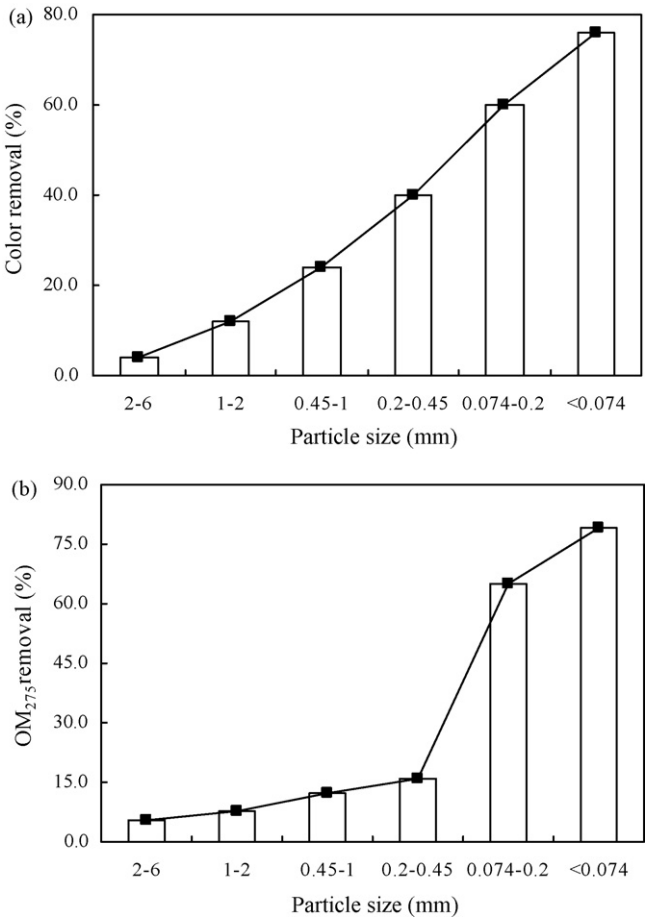

Fig. 4. Color removal for coking wastewater (a) and OM_{275} removal for papermaking wastewater (b) at 25 °C. Adsorbent dosage = 10 g/100 mL, pH = 8.75 (coking wastewater) and 8.73 (papermaking wastewater).

from 2–6 mm to 0.2–0.45 mm, and then rises significantly for 0.074–0.2 mm and <0.074 mm of bottom ash (Fig. 4(b)). Comparing Fig. 4(b) with Fig. 1, greater removal efficiencies of OM_{275} are observed than those of COD for papermaking wastewater. Especially for the bottom ash samples with smaller particle sizes, the maximum removal efficiency of OM_{275} is up to 79.0%, while that of COD is only about 40.6% for papermaking wastewater. This suggests that the aromatic organic matters are more easily removed by bottom ash than other kinds of organic components in papermaking wastewater.

Because of the relative higher removal efficiencies of COD, color, and/or OM_{275} for 0.074–0.2 mm and <0.074 mm of bottom ash, the following experiments were carried out only using these two different particle sizes of bottom ash.

3.2. Effect of bottom ash dosage

The effect of bottom ash dosage was investigated by increasing the dosage of bottom ash from 0.5 g/100 mL to 18 g/100 mL. Generally, similar trends (Fig. 5) are found for two different particle sizes of bottom ash (0.074–0.2 mm and <0.074 mm). It is found that the COD removal efficiency initially increases steeply, and then gradually with the increase of bottom ash dosage for coking wastewater (Fig. 5(a)). This is in agreement with previous studies [4,5,8,9,12]. The maximum COD removal efficiencies, 34.8% for 0.074–0.2 mm of bottom ash and 44.0% for <0.074 mm of bottom ash, are found at bottom ash dosage of 8 g/100 mL for coking wastewater.

However, two stages of the COD removal efficiency are observed with rising bottom ash dosages for papermaking wastewater (Fig. 5(b)). The COD removal efficiency increases gradually at bottom ash dosage lower than 8.0 g/100 mL, sharply at bottom ash dosage ranging from 8.0 g/100 mL to 12.5 g/100 mL, and then gradually. The maximum COD removal efficiencies, 27.8% for 0.074–0.2 mm of bottom ash and 45.8% for <0.074 mm of bottom ash, are obtained at bottom ash dosage of 12.5 g/100 mL for papermaking wastewater.

Comparing Fig. 5(a) with Fig. 5(b), different trends of COD removal efficiency with bottom ash dosage are observed for coking wastewater and papermaking wastewater. This may be ascribed to the various compositions of organic matters in these two kinds of wastewaters. From the chemical constituents of the bottom ash (Table 2), it is found that bottom ash is rich in aluminum and iron oxides, and their contents make up about 35.6% of the bottom ash. Both compounds are the essential raw materials for the production of water and wastewater treatment coagulants [17]. Therefore, besides adsorption bottom ash could remove organic matters, especially particle organic matters, in wastewater via coagulation due to its high contents of aluminum and iron oxides. At lower bottom ash dosage, coagulation may be the main mechanism for COD removal, and the adsorption mechanism becomes dominating with rising bottom ash dosage. Furthermore, the POC is mainly removed via coagulation, while

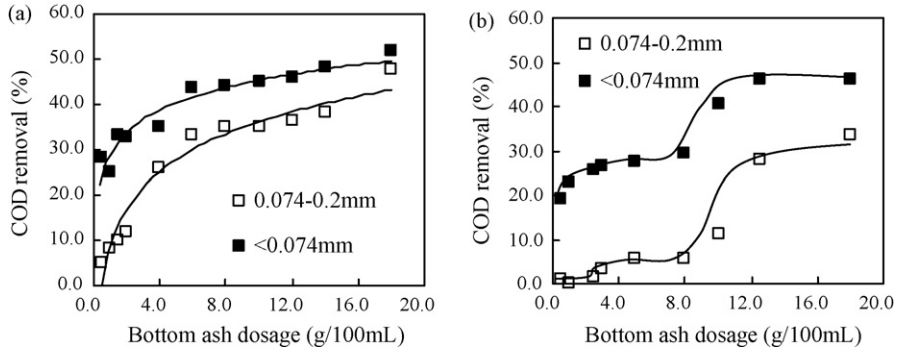

Fig. 5. COD removal at different bottom ash dosages. Temperature = 25 °C; (a) coking wastewater, pH = 8.75; (b) papermaking wastewater, pH = 8.73.

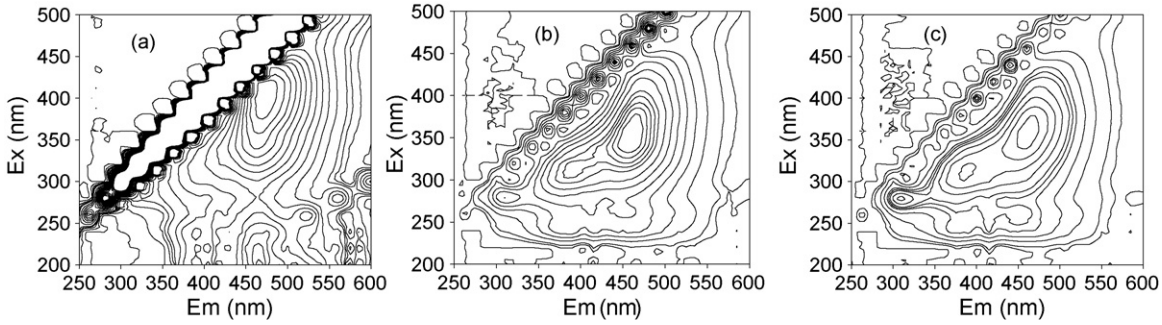

Fig. 6. FEEM spectra of coking wastewater: (a) raw coking wastewater, (b) after adsorption by 0.074–0.2 mm of bottom ash, (c) after adsorption by <0.074 mm of bottom ash.

most of the DOC is removed via adsorption. As shown in Fig. 2, the percentage of POC in TOC for papermaking wastewater is much lower than that for coking wastewater, and this may result in the two stages of the COD removal efficiency with rising bottom ash dosage for papermaking wastewater (Fig. 5(b)).

3.3. FEEM variations of wastewaters

Fig. 6 presents the fluorescence spectra of coking wastewater before and after treated by bottom ash. Significant variations are observed for the FEEM spectra of coking wastewater after adsorption by bottom ash. One intense excitation–emission peak, located at Ex/Em = 400 nm/470 nm, is observed for raw coking wastewater (Fig. 6(a)). After adsorption by bottom ash ((Fig. 6(b) and (c)), four typical excitation–emission peak are found, and they center at Ex/Em = 340–360 nm/460–470 nm, Ex/Em = 250–260 nm/440–450 nm, Ex/Em = 310–320 nm/390–400 nm, and Ex/Em = 280 nm/310 nm, respectively. Moreover, the lowest fluorescence intensities of these four peaks are observed for wastewater after adsorption by <0.074 mm of bottom ash due to its highest removal efficiency of COD (Fig. 1).

Similar to coking wastewater, evident changes are found for the FEEM spectra of papermaking wastewater after adsorption by bottom ash (Fig. 7). Two characteristic excitation-emission peak, located at Ex/Em = 340 nm/430 nm and Ex/Em = 280 nm/435 nm, are observed for raw papermaking wastewater (Fig. 7(a)). After adsorption by bottom ash ((Fig. 7(b) and (c)), three typical excitation-emission peak located at Ex/Em = 300 nm/380–390 nm, Ex/Em = 240 nm/390 nm, and Ex/Em = 240 nm/320–350 nm are found. Furthermore, the lowest fluorescence intensities of these three peaks are observed for wastewater after adsorption by <0.074 mm of bottom ash because of its highest removal efficiencies of COD and OM_{275} (Figs. 1 and 4(b)).

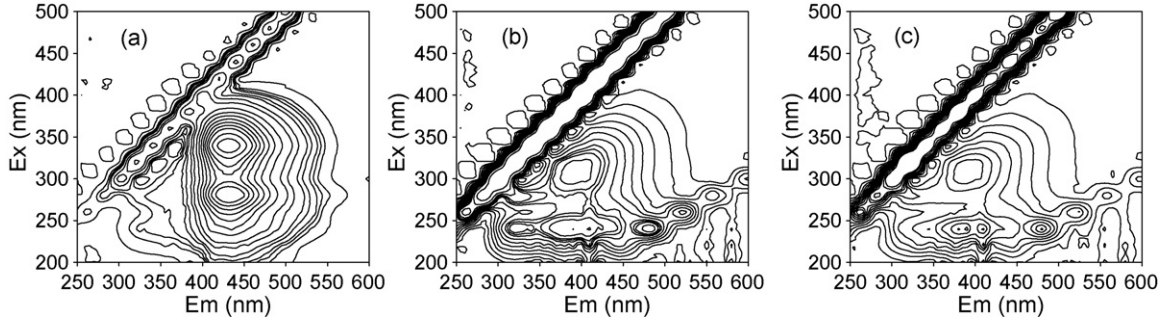

Fig. 7. FEEM spectra of papermaking wastewater: (a) raw papermaking wastewater, (b) after adsorption by 0.074–0.2 mm of bottom ash, (c) after adsorption by <0.074 mm of bottom ash.

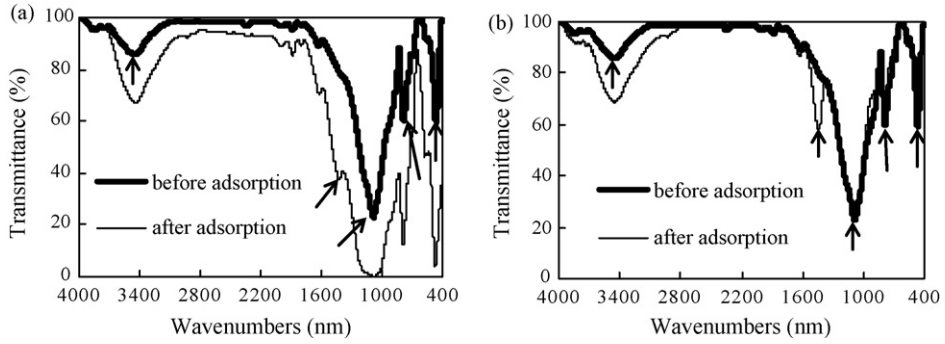

Fig. 8. FTIR spectra of bottom ash (particle size <0.074 mm) before and after adsorption: (a) coking wastewater, (b) papermaking wastewater.

Compared to coking wastewater (Fig. 6), it is found that the excitation wavelengths of fluorescence peaks observed for papermaking wastewater (Fig. 7) shift to UV light region. This suggests that the organic matters in papermaking wastewater are more prone to absorb UV light, while organic matters in coking wastewater are apt to absorb visible light. This also proves the results demonstrated in Fig. 3 that an absorption band is observed in the UV region and visible region for papermaking wastewater and coking wastewater, respectively. Moreover, different FEEM spectra of raw wastewaters (Fig. 6(a) and 7(a)) also confirm the various compositions of organic matters in coking wastewater and papermaking wastewater.

Although FEEM spectra, an easily measured method, has been widely used to determine the characteristics of organic matters in various samples [18,19], further researches on the relation between the organic components in water samples and its fluorescence characteristics should be made to explain the FEEM variations of wastewaters.

3.4. Variation of bottom ash characteristics

3.4.1. FTIR spectra

FTIR spectroscopy provides structural and compositional information on the functional groups presented in the samples. As illustrated in Fig. 8, the FTIR spectra of bottom ash show four typical broad transmittance bands in the region of 3450 cm^{-1}, 1065 cm^{-1}, 785 cm^{-1}, and 455 cm^{-1}. The band centered at 3450 cm^{-1} probably arises from H-bonded OH groups of water molecule, and can be attributed to interaction of the water hydroxyl with the cations; the strongest band centered at 1065 cm^{-1} may be due to vibrations of the internal tetrahedron ties Si–O–Si and Si–O–Al; the band at 785 cm^{-1} may represent the bending vibration of carbonate, means the presence of calcite or calcite with magnesium; the band at 455 cm^{-1} may result from Si–O–Si bending vibrations [20–23]. The peaks observed in the FTIR spectra confirm the presence of quartz, mullite, potash feldspar, plagioclase, and calcite in bottom ash. This is consistent with the chemical constituents and mineral components of bottom ash shown in Table 2.

After adsorption, an evident transmittance band in the region of 1400–1420 cm^{-1} is found in the infrared spectra of bottom ash. This band may be attributed to the –OH and –CO deformation from alcoholic and phenolic –OH, and –COO-symmetric stretch [20], and the organic pollutants containing these functional groups are widely exited in coking wastewater and papermaking wastewater. Lai et al. [2] found that the dominant compounds in coking wastewater after zero-valent iron treatment process were ester compounds. Ghoreishi and Haghighi [24] reported that more phenol compounds were produced in pulp and paper mill wastewater after biological treatment. The result demonstrated by Fig. 8 reveals that the organic pollutants in coking wastewater and papermaking wastewater are adsorbed by bottom ash.

3.4.2. SEM photographs

The SEM photograph of raw bottom ash (Fig. 9(a)) recognizes the surface of bottom ash granules is uneven, and reveals the porosity of the samples. The large fractions of bottom ash consist of either hollow spheres or hollow spheres packed with large numbers of smaller spheres. Microcrystals are also observed on the surface of the particles, and this may indicates the presence of mullite, quartz, and the typical plerospheres containing Si, Al, Ca, Na, and small amounts of Fe [25]. This is in accordance with the chemical constituents and mineral components of bottom ash illustrated in Table 2.

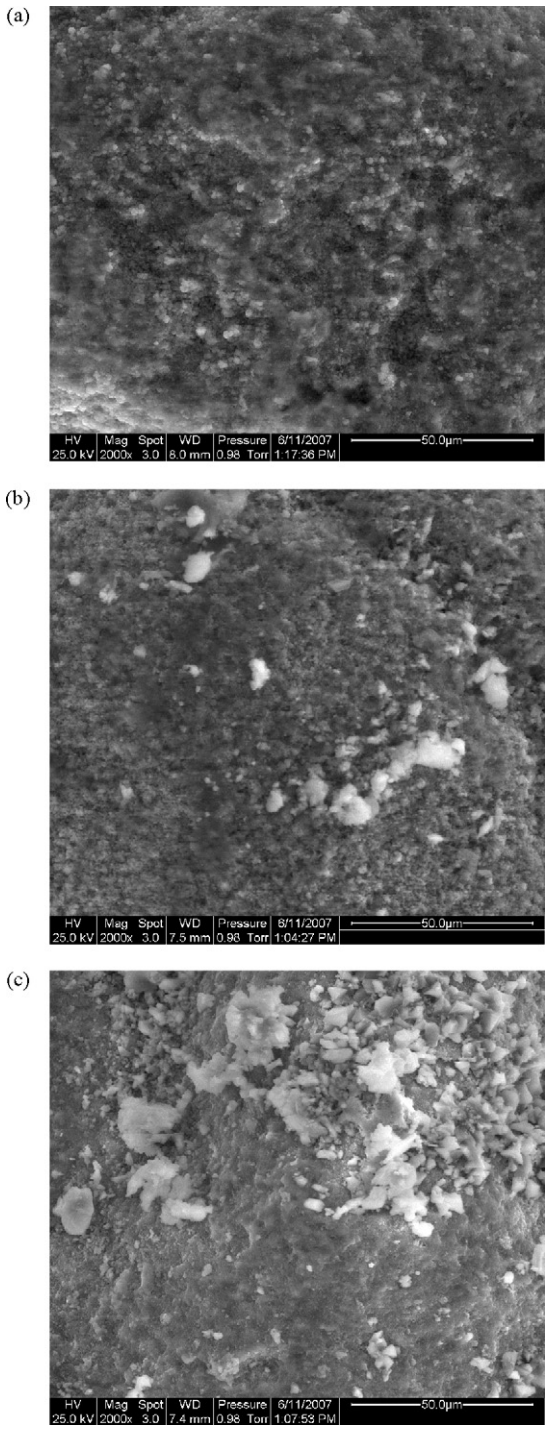

Fig. 9. SEM photographs of bottom ash (particle size <0.074 mm) at magnification of 2000: (a) raw bottom ash, (b) after adsorption of coking wastewater, (c) after adsorption of papermaking wastewater.

After adsorption (Fig. 9(b) and (c)), the surface of bottom ash particles varies significantly. A large numbers of small spheres disappear, and most of the hollow holes in bottom ash surface are packed with large amount of pollutants. Moreover, it appears that more evident changes for the configuration of bottom ash surface occur after adsorption of papermaking wastewater than after adsorption of coking wastewater. This may be related to the chemical components of these two kinds of wastewaters.

4. Conclusion

The COD removal efficiencies of wastewaters increase with decreasing particle sizes of bottom ash, and the COD removal efficiency for coking wastewater is much higher than that for papermaking wastewater due to its high percentage of particle organic carbon (POC). Under conditions of bottom ash dosage of 10 g/100 mL and <0.074 mm of particle size, it can achieve 45.0% COD removal and 76.0% color reduction for coking wastewater, and 40.6% COD removal and 79.0% OM_{275} reduction for papermaking wastewater. Different trends of COD removal efficiency with bottom ash dosage are observed for coking wastewater and papermaking wastewater due to their various compositions of organic matters. Significant variations are observed for the FEEM spectra of wastewaters after treatment by bottom ash. New excitation-emission peaks are found in FEEM spectra of wastewaters, and the fluorescence intensities of the peaks decrease. A new transmittance band in the region of 1400–1420 cm^{-1}, attributed to the organic matters containing –OH, –CO, or –COO– functional groups, is found in FTIR spectra of bottom ash after adsorption. The SEM photographs reveal that the surface of bottom ash particles varies evidently after adsorption. The experimental results underline the potential of bottom ash for the removal of organic pollutants from wastewaters. However, further investigation on column operations should be made to assess the practical utility of the bottom ash.

Acknowledgements

Financial support is from National Natural Science Foundation of China (Grant No. 40501063). The authors would like to thank the four anonymous reviewers for their constructive comments and suggestions.

References

[1] B.R. Lim, H.Y. Hu, K. Fujie, Biological degradation and chemical oxidation characteristics of coke-oven wastewater, Water Air Soil Pollut. 146 (2003) 23–33.
[2] P. Lai, H.Z. Zhao, C. Wang, J.R. Ni, Advanced treatment of coking wastewater by coagulation and zero-valent iron processes, J. Hazard. Mater. 147 (2007) 232–239.
[3] V.K. Gupta, A. Mittal, V. Gajbe, Adsorption and desorption studies of a water soluble dye, Quinoline Yellow, using waste materials, J. Colloid Interf. Sci. 284 (2005) 89–98.
[4] V.K. Gupta, A. Mittal, L. Krishnan, J. Mittal, Adsorption treatment and recovery of the hazardous dye, Brilliant Blue FCF, over bottom ash and de-oiled soya, J. Colloid Interf. Sci. 293 (2006) 16–26.
[5] V.K. Gupta, A. Mittal, L. Krishnan, V. Gajbe, Adsorption kinetics and column operations for the removal and recovery of malachite green from wastewater using bottom ash, Sep. Purif. Technol. 40 (2004) 87–96.
[6] A. Mittal, L. Kurup (Krishnan), V.K. Gupta, Use of waste materials—bottom ash and de-oiled soya, as potential adsorbents for the removal of Amaranth from aqueous solutions, J. Hazard. Mater. 117 (2005) 171–178.
[7] V.K. Gupta, Removal and recovery of the hazardous Azo Dye Acid Orange 7 through adsorption over waste materials: bottom ash and de-oiled soya, Ind. Eng. Chem. Res. 45 (2006) 1446–1453.
[8] A. Mittal, J. Mittal, L. Kurup, Adsorption isotherms, kinetics and column operations for the removal of hazardous dye, Tartrazine from aqueous solutions using waste materials—bottom ash and de-oiled soya, as adsorbents, J. Hazard. Mater. 136 (2006) 567–578.
[9] A. Mittal, J. Mittal, L. Kurup, Batch and bulk removal of hazardous dye, indigo carmine from wastewater through adsorption, J. Hazard. Mater. 137 (2006) 591–602.
[10] A. Mittal, J. Mittal, L. Kurup, A.K. Singh, Process development for the removal and recovery of hazardous dye erythrosine from wastewater by waste materials—bottom ash and de-oiled soya as adsorbents, J. Hazard. Mater. 138 (2006) 95–105.
[11] A.R. Dincer, Y. Gunes, N. Karakaya, Coal-based bottom ash (CBBA) waste material as adsorbent for removal of textile dyestuffs from aqueous solution, J. Hazard. Mater. 141 (2007) 529–535.
[12] A. Mittal, A. Malviya, D. Kaur, J. Mittal, L. Kurup, Studies on the adsorption kinetics and isotherms for the removal and recovery of Methyl Orange from wastewaters using waste materials, J. Hazard. Mater. 148 (2007) 229–240.
[13] A. Mittal, V. Gajbe, J. Mittal, Removal and recovery of hazardous triphenylmethane dye, Methyl Violet through adsorption over granulated waste materials, J. Hazard. Mater. 150 (2008) 364–375.
[14] A. Mittal, V.K. Gupta, A. Malviya, J. Mittal, Process development for the batch and bulk removal and recovery of a hazardous, water-soluble azo dye (Metanil Yellow) by adsorption over waste materials (bottom ash and de-oiled soya), J. Hazard. Mater. 151 (2008) 821–832.
[15] Metcalf & Eddy, Inc., Wastewater Engineering: Treatment and Reuse, fourth ed., McGraw-Hill Companies, Inc. (reprint by Tsinghua University Press), Beijing, 2003.
[16] W.L. Sun, J.R. Ni, T.T. Liu, Effect of sediment humic substances on sorption of selected endocrine disruptors, Water Air Soil Pollut.: Focus 6 (2006) 583–591.
[17] M. Fan, R. Brown, T.D. Wheelock, A.T. Cooper, M. Nomura, Y. Zhuang, Production of a complex coagulant from fly ash, Chem. Eng. J. 106 (2005) 269–277.
[18] A. Baker, Fluorescence excitation–emission matrix characterization of some sewage-impacted rivers, Environ. Sci. Technol. 35 (2001) 948–953.
[19] W.L. Sun, J.R. Ni, N. Xu, L.Y. Sun, Fluorescence of sediment humic substance and its effect on the sorption of selected endocrine disruptors, Chemosphere 66 (2007) 700–707.
[20] W.M. Davis, C.L. Erickson, C.T. Johnston, J.J. Delfino, J.E. Porter, Quantitation Fourier transform infrared spectroscopic investigation of humic substance functional group composition, Chemosphere 38 (1999) 2913–2928.
[21] A. Özcan, A.S. Özcan, Adsorption of Acid Red 57 from aqueous solutions onto surfactant-modified sepiolite, J. Hazard. Mater. 125 (2005) 252–259.
[22] F.M. Martins, J.M. Martins, L.C. Ferracin, C.J. Cunha, Mineral phases of green liquor dregs, slaker grits, lime mud and wood ash of a Kraft pulp and paper mill, J. Hazard. Mater. 147 (2007) 610–617.
[23] M. Sprynskyy, T. Ligor, B. Buszewski, Clinoptilolite in study of lindane and aldrin sorption processes from water solution, J. Hazard. Mater. 151 (2008) 570–577.
[24] S.M. Ghoreishi, M.R. Haghighi, Chromophores removal in pulp and paper mill effluent via hydrogenation-biological batch reactors, Chem. Eng. J. 127 (2007) 59–70.
[25] Y.-S. Shim, Y.-K. Kim, S.-H. Kong, S.-W. Rhee, W.-K. Lee, The adsorption characteristics of heavy metals by various particle sizes of MSWI bottom ash, Waste Manage. 23 (2003) 851–857.